Electronic Supplementary Material (ESI) for Soft Matter.

Supplementary Information: Colloidal Crystallites Under External Oscillation

Hreedish Kakoty[1], Yunhu Huang[2], Rajarshi Banerjee[1], Chandan Dasgupta[1,3], and Ambarish Ghosh[*1,2]

[1] *Department of Physics, Indian Institute of Science, Bangalore 560012, India*
[2] *Centre for Nano Science and Engineering, Indian Institute of Science, Bangalore 560012, India*
[3] *International Centre for Theoretical Sciences, Bangalore 560089, India*

Contents

[*]Corresponding author

1 Description of Movies

M1: Movie of formation of crystallite with polystyrene beads of diameter 1 μm. The Z level of the sample plane was 6.4 μm below the focal plane. The crystalline transition was observed as laser power was increased from $99mW$ to $105mW$. The movie was captured at 148 fps with a CCD camera.

M2: Movie of a crystallite under oscillation with amplitude of 1 μm at frequency $1Hz$.

M3: Color plot movie of the local bond orientational order ϕ_6 for small amplitudes of oscillation as described in Fig. 2 of the main manuscript.

M4: Experimental crystallite under a large amplitude of oscillation (5 μm) at $1Hz$ as described in Fig. 3a of the main manuscript.

M5: Movie of a simulated crystal with a harmonic confinement extending to infinity. (Fig. 3b of main manuscript)

M6: Movie of a simulated crystal with a confinement potential which is harmonic at the centre and has exponential decay towards the edges. (Fig. 3c of main manuscript, section 5 of supplementary)

M7: Movie of a simulated crystal with a confinement potential which is harmonic at the centre and has two different exponential decay along the axis of oscillation (X axis). (Fig. 3d of main manuscript, section 5 of supplementary)

2 Details of the Experimental Setup

The microfluidic cell for our experiments is made using a thick glass slide and a much thinner glass cover slip. Colloidal particles used in the experiments are 1 μm Polystyrene beads from Spherotech. As specified by the vendor, the coefficient of variation of the particle diameter was around 12%, and experimentally we could not observe much irregularity either. These colloidal particles are diluted in DI water and a drop of solution of about 4 μL is allowed to spread evenly between the glass slide and cover slip. The edges of the microfluidic cell is sealed by using a superglue. As shown in the schematic(Fig. 2a), the cover slip has a side length of 2 cm. It has a square cross-section. The amount of solution used to make the microfluidic chamber was 4 μL, which was carefully measured before making the microfluidic chamber. This volume of solution spread around an area of 4 cm^2 gives us a net thickness of 10 μm. The surfaces of the chamber were extensively cleaned beforehand, which ensured uniform spreading of the solution. The uniform spreading ensured no air was trapped to form bubbles; however, in case there was a bubble formed, we discarded the chamber. The spreading varied by a small amount every time, which corresponded to small variation in thickness of the chamber. All these procedures were

necessary to achieve a thickness of 10 μm. This small thickness ensured that in our experiments the colloidal particles stabilized at one particular Z-level, due to gravity and repulsion from the two glass slides (electrostatic)(Fig. 2a).

The thickness of the cell was measured by the following method: we used a diamond cutter to make a small scratch on the inside of the cover slip (side facing the colloidal solution) and the glass slide (side facing the colloidal solution). After we make the microfluidic cell, we placed it under our microscope and focussed our objective lens on the scratch mark on the cover slip first. Then we move our objective lens upward with precision of 1 μm (Olympus Microscope IX71) and focus on the scratch mark on the top glass. The vertical distance traversed by the objective lens, as seen from the objective translation wheel tells us the height of the microfluidic cell. We have observed that if we maintained the solution spreads evenly throughout the glass cover slip, we see a vertical height of 10 μm with precession error of ± 1 μm. This uniformity goes away for small number of bubbles or empty spaces left inside the cell and then the cell was discarded. We have also observed some variation of this thickness towards the edges where the cover slip is stuck to the glass slide using a superglue. However, this variation is small (± 1 μm in most cases) and our experiments are carried out near the centre of the microfluidic cell, hence we have a uniform thickness of 10 ± 1 μm in our region of interest.

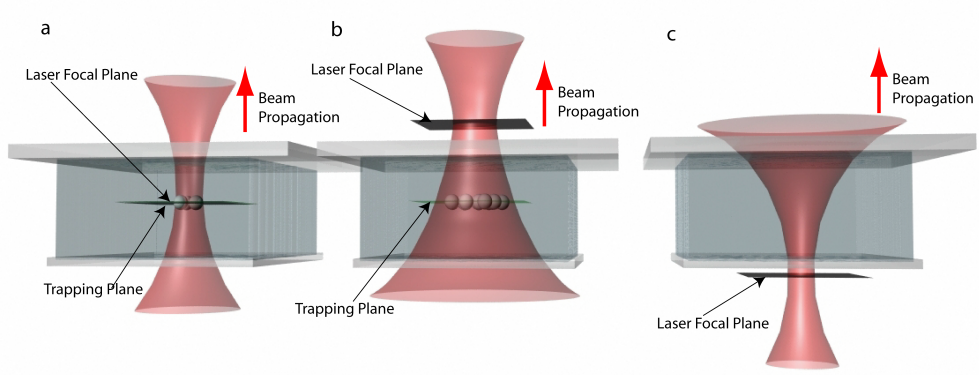

Figure 1: Different defocussing levels

Three different defocusing configurations in Fig. 1-(a) The laser focal plane and the optical trapping plane are at the same Z level. (b) Laser focal plane is above the optical trapping plane. (c) Laser focal plane is below the plane of untrapped beads. The Z position of the trapped colloidal assembly is determined by four forces acting on the beads; radiation pressure from the laser beam pushing the particles upward, gradient force along $\hat{Z}$ pulling the beads towards the focus, downward repulsion from the charged glass surface and gravity. In (a) when gradient force of the beam along $\hat{Z}$ is almost 0 the radiation force, the surface repulsive force and the weight create a stable trap. In (b) when the gradient force as well as radiation force act in the upward direction, the surface repulsive force and the weight balance it to create a stable trap. But in (c) the gradient force is in the downward direction whereas the other three forces do not change sign. In this configuration the forces do not balance to give stable trapping and hence no trapping could be seen.

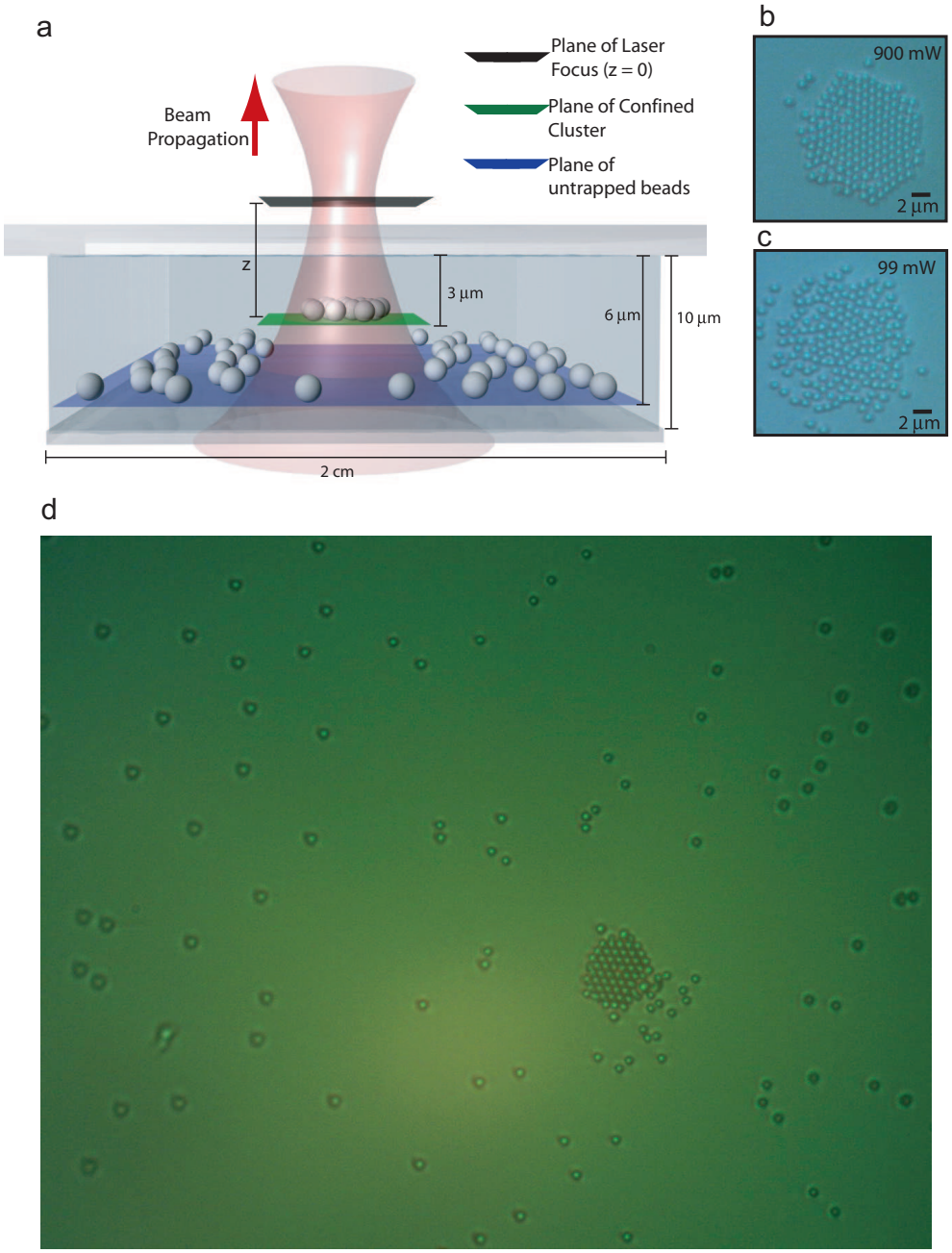

Figure 2: (a) Schematic of the experimental setup [1]: Laser beam focused at a plane higher (along $\hat{Z}$) than the plane of observation containing the colloidal assembly. The confinement along $\hat{Z}$ was obtained due to the balance of forces described Fig. 1, resulting in a finite sized two-dimensional colloidal cluster (b) Colloidal assembly when focusing the laser beam at a distance of 6.4 μm above the sample plane 900 mW (c) Reducing the laser power to 99 mW while focusing at the same position ($z = 6.4$ μm,) results in a disordered (liquid-like) assembly of the same size as the crystallite (d) Image of the colloidal dispersion of larger area inside the microfluidic chamber using a lower magnification zoom lens, which shows the colloidal particles inside the colloidal crystal being in a different focus compared to those outside the laser beam waist

In the absence of the laser beam, the colloidal layer stabilizes at 6 μm from the top

glass surface, due to gravity and the electrostatic repulsion from the two glass surfaces. Once the laser is irradiated, due the additional forces of radiation pressure in the direction of propagation (upward) and the Z gradient force towards the laser focus (upward), the particles within the beam waist gets a push upward. The balance of these forces makes it stabilize at 3 μm from the top glass surface.

In order to estimate the vertical height of the colloidal particles we made scratch marks on the glass surfaces to locate the Z height of each surface by focussing the objective on these marks. We first focus our objective on the lower scratch mark on the cover slip. Then we slowly move the objective upward and focus the floating particles and observed the Z distance by which the objective has been moved in order to reach the focal plane of the colloids. This gave us a good estimate of the height of the floating particles, which we have measured to be 4 μm. As soon as the laser was turned on we observed the particles inside the beam waist to go out of focus. We again moved the objective upward by a certain distance to focus on these particles, and estimated the change in Z height from the movement of the objective. We observed that the particles went up by about 3 μm compared to the Z level without the optical trap.

The glass slide and the cover slip used in our experiments are cleaned and treated with piranha solution (3 parts sulphuric acid and 1 part hydrogen peroxide). Treatment with piranha hydroxylates the glass surfaces and makes the glass surfaces negatively charged because of the OH group. The surface of the polystyrene particles we use are also negatively charged, which is also specified by Spherotech. Because of this electrostatic repulsion the polystyrene particles cannot completely fall to the bottom surface due to gravity. We have measured this height to be 4 μm from the bottom surface, by varying the focal plane as described before.

A similar observation was made by Sun et al [2] where they observed simultaneous optical trapping of microparticles in different planes using modified self-imaging technique. In their study they made a microfluidic chamber of thickness 70 μm where they reported a mixture of silica and polystyrene particles to be suspending at the same plane several microns above the bottom glass slide. By the use of an array of optical traps they were able to vertically separate the silica and polystyrene particles into two planes based on the radiation pressure.

Another study made by Vossen et al [3] showed that a concentrated dispersion of 1.4 μm silica particles in a 100 μm thick capillary, observed with confocal microscopy was seen to be only a few microns thick. By using a defocused optical trap with low numerical aperture objective they also showed 3D images of the bead dispersion being pushed against the glass slide along the direction of the propagation of laser.

Here we provide an experimental image with a lower zoom lens(Fig. 2d), showing an extended area in the microfluidic cell, where we clearly see the particles inside the optical trap (see the colloidal crystal) being in focus and particles around the trap being out of focus.

3 Estimating the trap constant from position fluctuations

Thermally driven position fluctuations can give us information about the potential energy of the optical trap. We placed a single polystyrene bead near the centre of the trap and

looked at its Brownian fluctuations. In equilibrium, we expect the probability density of the particle position to be described by Boltzmann statistics. Considering the confining potential to be harmonic near the centre, we can write this probability density for two dimensional confinement as

$$\rho(x,y) = C\ \exp\left(-\frac{k_x x^2}{2k_B T} - \frac{k_y y^2}{2k_B T}\right), \tag{1}$$

where k_x and k_y are the spring constants for motion in the x and y directions, respectively. This Gaussian distribution relates the mean-square displacement to the trap constant:

$$\langle x^2\rangle = \frac{k_B T}{k_x},\ \langle y^2\rangle = \frac{k_B T}{k_y}, \tag{2}$$

These relations represent the equipartition theorem for each quadratic degree of freedom. We calculated the variance in the position of the bead at different laser powers for a large optical trap ($Z = 6.4\ \mu$m) and obtained a dimensionless trap energy parameter for our system,

$$\frac{U_{trap}}{k_B T} = \frac{1}{2}\frac{ka^2}{k_B T}, \tag{3}$$

where $k_x = k_y = k$, $a = 1\ \mu$m, $T = 300$ K. This parameter is plotted as a function of the laser power in Fig. 3.

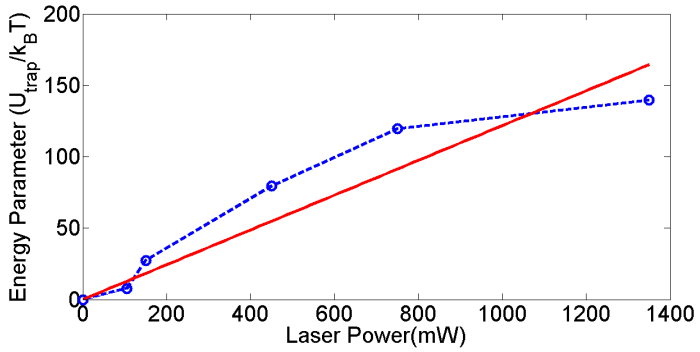

Figure 3: Variation of trap energy parameter($U_{trap}/k_B T$) with laser power. The linear fit was made with a constraint of zero intercept. The slope was found to be 0.13 mW^{-1}.

We have verified that our acquisition time for fluctuation study is sufficient. We have plotted the width of the Gaussian distribution as a function of sampling time and have verified that the FWHM reaches a plateau in a timescale much less than our measurement time.

4 Local Bond Orientational Order of the Crystallites

As shown in Fig. 1c of the main manuscript there is a difference between the highest global bond orientational order parameter ($|\psi_6|$) in our experiments and simulation. The

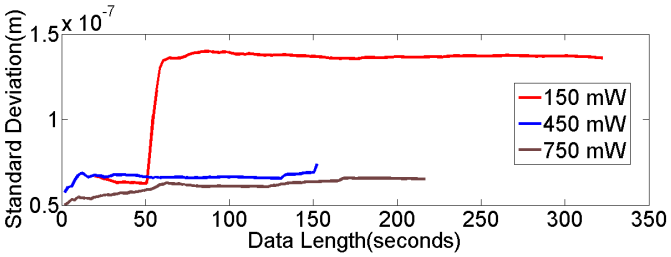

Figure 4: The plot shows that the FWHM of the Gaussian distribution of the particle position reaches a constant value in timescales much less than our experimental timescale.

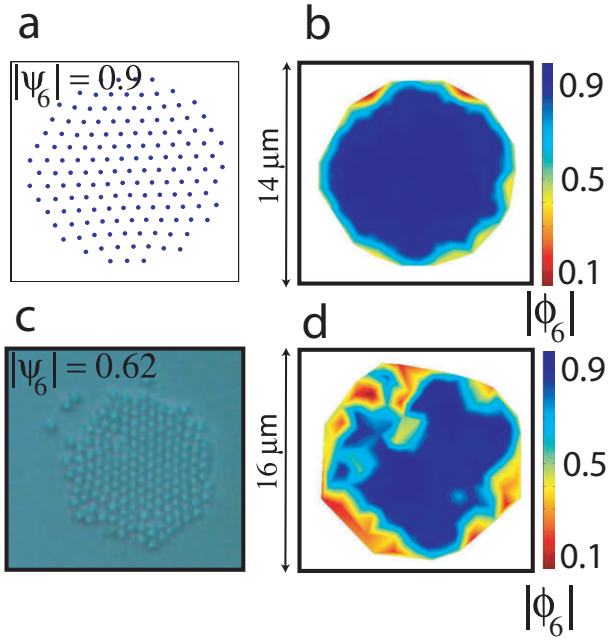

Figure 5: (a),(c) Snapshots of the simulated and experimental crystals and their corresponding $|\psi_6|$. (b),(d) Local bond-orientational order parameter $|\phi_6|$ of the crystals in (a) and (c) respectively.

highest $|\psi_6|$ observed in simulations was 0.9 whereas the highest achieved in experiments was 0.69. This difference is probably related to the experimental trapping potential being more uneven towards the edges which makes the particles on the edges of experimental crystal more disordered. To verify this we compare the local bond-orientational order parameter $|\phi_6|$ of simulated and experimental crystals.

As can be seen from Fig. 5b and 5d, the $|\phi_6|$ values match very well for simulations and experiments in the bulk of the crystal ($|\phi_6| = 0.9$). But the edges of the experimental crystals have very low values of $|\phi_6|$ which reduces the global order of the experimental crystal as compared to our simulations.

5 Correction to the Confinement Potential

As mentioned in the main manuscript, at higher amplitudes of oscillation our simulations showed deviations from the experimental picture where one side of the oscillation elongated the crystal more than the other. A harmonic confinement could not provide an explanation as in this case there was no deformation seen in the crystal for any amplitude. As a first correction we assumed an exponential decay of the potential towards the edges.

$$V = \frac{1}{2}k(r^2 - R_e^2) - V_{\text{off}}, r < R_e$$

$$V = -V_{\text{off}}\, e^{-(r-R_e)b}, r > R_e$$

$$b = \frac{kR_e}{V_{\text{off}}}$$

In this case, $k = 3 \times 10^{-8}\,\text{N/m}$, $R_e = 5.75\,\mu\text{m}$, $V_{\text{off}} = 60\ k_bT$, $T = 300\,\text{K}$, and k_b is the Boltzmann constant.

Though this case was closer to the experimental scenario it still did not give the exact picture of the asymmetric deformation on two sides of the oscillation. As a further correction we assumed the potential to have two different exponential decay along the axis of oscillation (X axis, Fig. 3d of Manuscript). We assumed $R_{e+} = 7.75\,\mu\text{m}$ towards positive X axis and $R_{e-} = -3.5\,\mu\text{m}$ along negative X axis. These potentials are plotted in Fig. 6 along with the experimental potential.

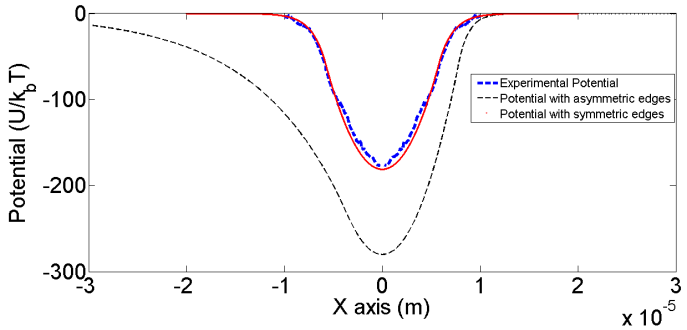

Figure 6: The figure shows the experimental potential(blue dotted line), the first approximation with exponential decay on both sides(red curve) and second correction with two different exponential decay on two sides of the oscillation axis(black dotted line).

References

[1] Hreedish Kakoty, Rajarshi Banerjee, Chandan Dasgupta, and Ambarish Ghosh. Role of entropy in the expulsion of dopants from optically trapped colloidal assemblies. *Phys. Rev. Lett.*, 117:258002, Dec 2016.

[2] Y. Y. Sun, J. Bu, L. S. Ong, and X.-C. Yuan. Simultaneous optical trapping of microparticles in multiple planes by a modified self-imaging effect on a chip. *Applied Physics Letters*, 91(5):051101, 2007.

[3] Dirk L. J. Vossen, Astrid van der Horst, Marileen Dogterom, and Alfons van Blaaderen. Optical tweezers and confocal microscopy for simultaneous three-dimensional manipulation and imaging in concentrated colloidal dispersions. *Review of Scientific Instruments*, 75(9):2960–2970, 2004.